Received: 6 May 2023 | Revised: 30 May 2023 | Accepted: 9 June 2023

DOI: 10.1002/agt2.373

Aggregate WILEY Open Access

RESEARCH ARTICLE

# Emission or scattering? Discriminating the origin of responsiveness in AIEgen-doped smart polymers using the TPE dye

**Valentina A. Dini**[1] | **Damiano Genovese**[1,2] | **Cosimo Micheletti**[3] | **Nelsi Zaccheroni**[1,2] | **Andrea Pucci**[3,4] | **Chiara Gualandi**[1,2,5,6]

[1]Department of Chemistry "Giacomo Ciamician", University of Bologna, Bologna, Italy

[2]INSTM UdR of Bologna, University of Bologna, Bologna, Italy

[3]Department of Chemistry and Industrial Chemistry, University of Pisa, Pisa, Italy

[4]INSTM UdR of Pisa, University of Pisa, Pisa, Italy

[5]Health Sciences and Technologies (HST) CIRI, University of Bologna, Ozzano Emilia Bologna, Italy

[6]Advanced Applications in Mechanical Engineering and Materials Technology CIRI, University of Bologna, Bologna, Italy

**Correspondence**
Chiara Gualandi, Department of Chemistry "Giacomo Ciamician", University of Bologna, Bologna, Italy.
Email: c.gualandi@unibo.it

**Funding information**
Ministero dell'Università e della Ricerca, Grant/Award Number: 20179BJNA2

**Abstract**

Aggregation-induced emission (AIE) luminogens are attractive dyes to probe polymer properties that depend on changes in chain mobility and free volume. When embedded in polymers the restriction of intramolecular motion (RIM) can lead to their photoluminescence quantum yield (PLQY) strong enhancement if local microviscosity increases (lowering of chain mobility and free volume). Nonetheless, measuring PLQY during stimuli, i.e. heat or mechanical stress, is technically challenging; thus, emission intensity is commonly used instead, assuming its direct correlation with the PLQY. Here, by using fluorescence lifetime as an absolute fluorescence parameter, it is demonstrated that this assumption can be invalid in many commonly encountered conditions. To this aim, different polymers are loaded with tetraphenylenethylene (TPE) and characterized during the application of thermal and mechanical stress and physical aging. Under these conditions, polymer matrix transparency variation is observed, possibly due to local changes in refractive index and to the formation of microfractures. By combining different characterization techniques, it is proved that scattering can affect the apparent emission intensity, while lifetime measurements can be used to ascertain whether the observed phenomenon is due to modifications of the photophysical properties of AIE dyes (RIM effect) or to alterations in the matrix optical properties.

**KEYWORDS**

AIE luminogens, glass transition, mechanochromism, physical aging, scattering, smart polymer

## 1 | INTRODUCTION

In a world where the use of plastics is becoming increasingly common in everyday life, the possibility of detecting damage and changes in properties of materials subjected to different surrounding environments becomes crucial. Therefore, interest in smart materials has increased drastically in recent years due to their ability to respond to an external stimulus by changing their physical, chemical or optical properties.[1–3] Common stimuli to which they are sensitive are temperature,[4] pH[5] and mechanical stress.[6,7] Given the ease and flexibility of light manipulation, obtaining an optical signal in response to a stimulus is particularly attractive, and among optical properties luminescence stands out for its high sensitivity and ease of detection. Changes in emission colour, intensity or lifetime, can be obtained by adding a suitable photoactive compound to a polymer matrix, either chemically bounded[8] or dispersed.[9] Luminophores known as AIE (aggregation-induced emission)[10] are often used for this purpose. They are characterized by a high quantum yield when the microenvironment restricts their intramolecular motions (RIM effect) or when in the solid state. As a result, whether they form aggregates or are embedded in a rigid matrix, the non-radiative decay pathways are deactivated, making the luminophore highly emissive.[11,12] Furthermore, by increasing their concentration, the sensitivity

of detecting their signal can be increased without the risk of quenching. Hence, structural features of the matrix, such as morphological or conformational variations, can be identified by investigating the emissive behaviour of the AIE[13–15] making them highly promising for the development of stimuli-responsive materials.[16]

Tetraphenylethylene (TPE), the simplest and most common AIE, has been frequently used in combination with various polymeric matrices to endow materials with different new functionalities. In this framework, TPE has been simply blended with the polymer[17–19] included in microcapsules dispersed in a polymer matrix,[20,21] covalently bound to the macromolecular chains,[22] or confined into a specific ply of a multilayer structure.[23,24] For instance, Robb et al. exploited the RIM effect to visually detect, under appropriate excitation light, microscopic damages in a wide range of polymers: in the crack region, TPE is released from solvent-containing microcapsules and, after solvent evaporation, TPE aggregation leads to a prominent fluorescence.[20] Meng et al. found a correlation between polymer tensile deformation and TPE emission intensity.[25] Used as an additive, TPE has also been proposed as a probe for polymer glass transition temperature ($T_g$)[17] and for the topology freezing transition temperature ($T_v$) in vitrimers.[26] Here, the decrease in TPE fluorescence intensity upon heating has been attributed to the change in mobility that occurs during the polymer transition. The starting assumption is that the rigidity of glassy polymer chains blocks TPE intramolecular motions, thus stronger emission is observed at temperatures below polymer $T_g$. By increasing the temperature above $T_g$, polymer chains acquire mobility and intramolecular motions in TPE are allowed with a consequent decrease in its emission. Similarly, in vitrimers, the polymer acquires dynamism and mobility when overcoming the $T_v$.

However, it is always important to consider that the observed luminescence of fluorophore-doped solid matrix, featuring only variations of the intensity, can be strongly influenced by the optical properties of the material, and in particular by scattering phenomena, frequently occurring as a consequence of refractive index discontinuities within the sample. These may originate from sample inhomogeneities such as local density variations, microcracks or microbubbles. Emission intensity can be massively affected by scattering, which can produce apparent enhancements of the emission signal. Therefore, the mere measurement of fluorescence emission intensity, without any investigation of the emission quantum yield, might be insufficient in some conditions and might lead to misleading results and conclusions. Emission intensity is indeed a relative measurement of quantum yield, valid only when the optical system under measurement, including geometry, absorption and scattering, does not change. As a consequence, it is crucial to measure also parameters not affected by the matrix scattering, to explain the observed phenomena on the basis of more reliable data. Unlike emission intensity, fluorescence lifetime is an inherent property of a fluorophore, with an absolute (and not a relative) value that is neither affected by scattering phenomena nor by the method of measurement.[27] Indeed, lifetime is directly proportional to the quantum yield (Equations (1) and (2)) when the quenching mechanisms involve only a variation of the non-radiative decay kinetics $k_{nr}$, as in the case of the RIM mechanism in AIEgens.

$$\tau = 1/\left(k_r + \sum_i k_{nr,i}\right) \quad (1)$$

$$\Phi = k_r/\left(k_r + \sum_i k_{nr,i}\right) \quad (2)$$

Therefore, in complex experimental conditions, including low-scattering optical systems, measuring the lifetime stands out as an easy way to evaluate the quantum yield.

This work aims to assess the photophysical properties of TPE dispersed in different polymeric microenvironments subjected to temperature variation, physical aging and mechanical deformation, by independent emission spectroscopy measurements, transmittance, imaging, and time-resolved spectroscopy measurements. The final intent is to verify the effect of scattering on TPE emission and better elucidate the mechanism behind the use of this AIE fluorophore in polymer properties detection. To this aim, TPE was dispersed in three different commercially available polymers, that is, poly(lactic-*co*-glycolic acid) (PLGA), polyvinyl acetate (PVAc) and polycarbonate (PC). These polymers, being completely amorphous materials with different $T_g$ values, were chosen to investigate the TPE emission properties under temperature variation. Being tough and highly deformable, PVAc was also tested under mechanical stretching.

## 2 | RESULTS AND DISCUSSION

### 2.1 | Investigation of the thermoluminochromic response

The polymers under investigation, that is, PVAc, PLGA, and PC, processed as depicted in Figure 1, were specifically selected for this study since they are completely amorphous and with glass transition temperatures falling in different temperature ranges. Figure 2A shows the second DSC scans of the TPE-doped polymer matrices from which the $T_g$ values were derived (i.e. 39, 47, and 148°C for PVAc, PLGA, and PC, respectively). We verified that no remarkable changes in the $T_g$ of the polymers are observed after the addition of the TPE (Figure S1 and Table S1), meaning that the TPE does not affect polymer thermal properties, at least in the amount used in the present work.

To determine fluorescence variation over temperature, UV light-irradiated samples were heated at a rate of 5°C min$^{-1}$. Figure 2B–D show the fluorescence intensity behaviour of the analyzed matrices as a function of temperature. The emission intensity was quantitatively expressed by the grayscale values obtained from the digital images, as previously reported by Qui et al.[28] and Meng et al.[25] Images of the tested polymers at different temperatures are also reported for each polymer. In the case of PVAc and PLGA, the almost complete quenching of the sample emission is obtained reaching 100°C, whereas, for PC, which has a higher $T_g$, only at

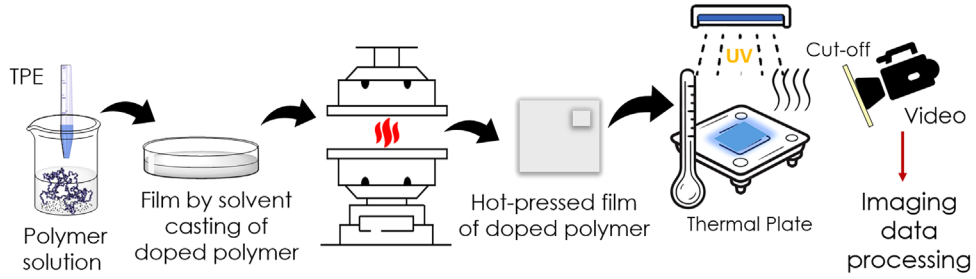


**FIGURE 1** Scheme of the experimental setup for the measurement of sample fluorescence variation under thermal treatment: Polymer films doped with TPE were obtained by solvent casting followed by hot-pressing; a specimen was positioned over a heating stage to carry out heating/cooling treatments under a controlled rate; the specimen was irradiated with UV light and the sample emission was monitored with a camera; images were processed by analyzing greyscale intensity, using ImageJ software.

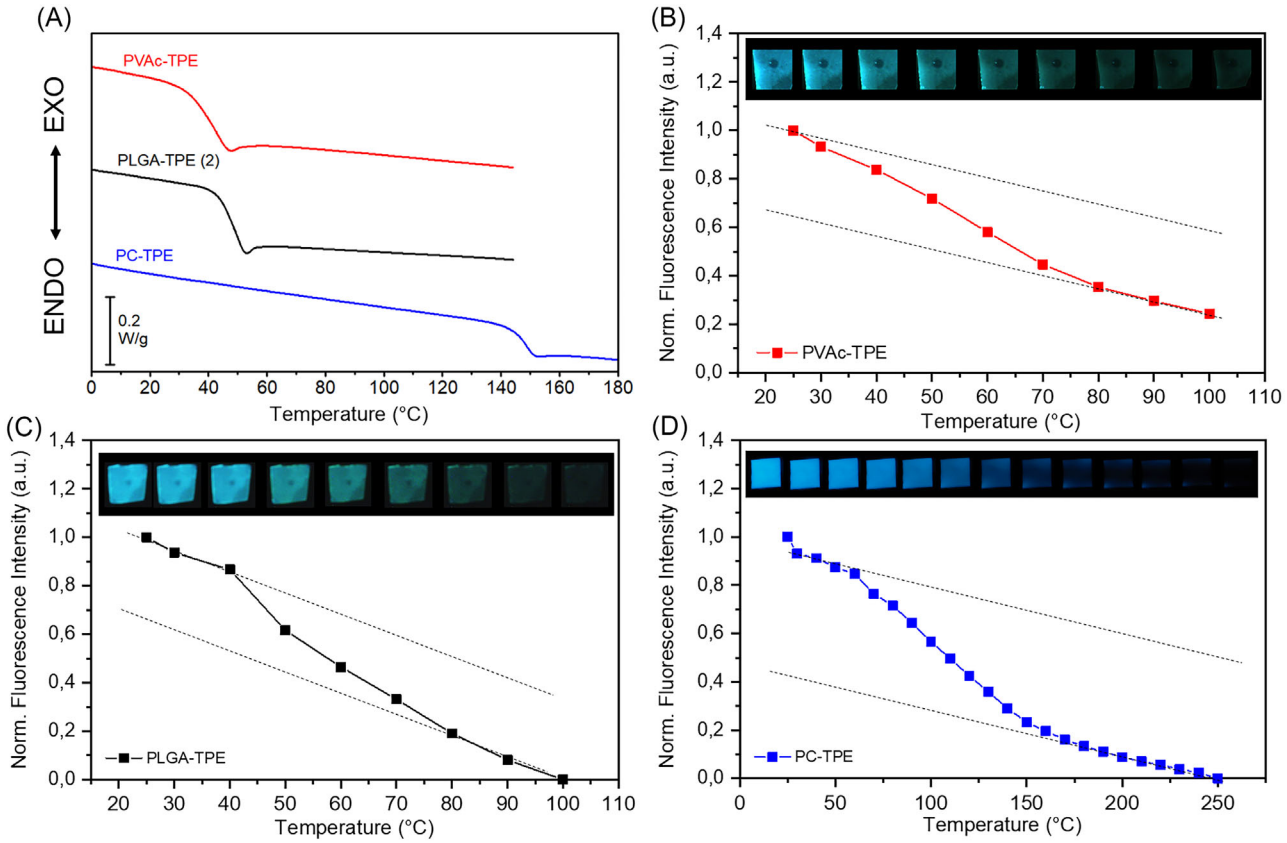


**FIGURE 2** (A) DSC second heating scans of PVAc-TPE (red), PLGA-TPE (black), and PC-TPE (blue). Fluorescence as a function of temperature, obtained from greyscale intensity analysis of TPE-doped sample images: (B) PVAc-TPE, (C) PLGA-TPE, and (D) PC-TPE. Dotted lines are added to better highlight the step-like change of sample emission across $T_g$. Images of samples acquired at different temperatures are also reported in sequence.

around 250°C. By observing sample images and graphs in Figure 2, it is evident that emission intensity decreases with temperature and that the greatest fluorescence variation occurs across polymer $T_g$, where a step-like change of the emission is observed. This temperature-dependent change in fluorescence can be reasonably ascribed to the RIM effect. Since the emission quantum yield of TPE is directly related to its mobility, below polymer $T_g$, where chains are vitrified in a random coil conformation, a higher quantum yield of TPE is expected, as a consequence of the RIM effect, in comparison with that above $T_g$, where chain mobility and free volume strongly increase together with the dye intramolecular motions.[13,29]

In order to get a deeper understanding of the fluorescence changes across polymer $T_g$, physical aging, a common phenomenon of the amorphous state, has been considered. Physical aging is a thermodynamic phenomenon whereby the material approaches a state of equilibrium through structural relaxations that slowly reduce the excessive free volume and cause volume contraction. This phenomenon occurs at temperatures below $T_g$ and is thermoreversible since, by heating the polymer above $T_g$, the free volume lost during aging is recovered.[30] The occurrence of physical aging is expected to reduce the free volume available for the AIE rotational motions, thus enhancing its radiative deactivation. In other words, TPE is expected to be sensitive to polymer

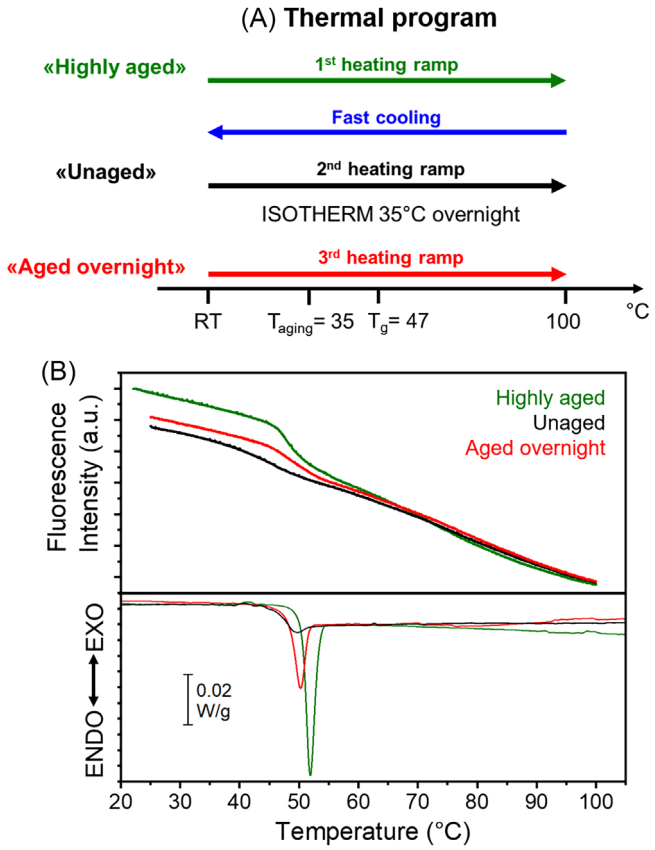


**FIGURE 3** (A) Thermal program applied to PLGA-TPE sample: the starting "highly aged" specimen was heated above $T_g$ and quickly cooled to gain the "unaged" sample, the latter, after being heated above $T_g$, was maintained at 35°C overnight to induce physical aging ("aged overnight" sample) and heated again to monitor its fluorescence. (B) Normalized variation of greyscale in terms of fluorescence intensity as a function of temperature for the differently aged PLGA samples; the corresponding DSC heating scans are also reported.

densification due to physical aging, as we previously reported for a phosphorescent AIE dye.[31]

To verify this hypothesis, TPE-doped PLGA, which shows the clearest fluorescence variation in correspondence to its $T_g$ among the tested polymers, was selected and subjected to cycles of heating, cooling and isotherm, as described in Figure 3A, while measuring fluorescence emission by grayscale analysis. In detail, a "highly aged" sample of PLGA-TPE, obtained by storing the polymer at room temperature for several weeks, was heated above its $T_g$ (1st heating ramp, Figure 3A, green segment) and quickly cooled (fast cooling ramp, Figure 3A, blue segment) to erase its thermal history and gain an "unaged" sample. The latter was subsequently re-heated (2nd heating ramp, Figure 3A, black segment). The same sample was then "aged overnight" at 35°C on the heating stage before being heated above its $T_g$ (3rd heating ramp, Figure 3A, red segment). During these thermal treatments, the camera continuously recorded the sample fluorescence. In parallel, the sample was also characterized by DSC to identify the $T_g$ and the extent of physical aging.

Figure 3B shows the change in sample fluorescence during the above-described heating scans, together with the corresponding DSC scans. In the latter, the step-change in the heat flow ascribable to the glass transition is overlapped with the enthalpic relaxation peak caused by the physical aging. As expected, the highly aged sample shows the more intense peak, followed by the sample aged overnight and by the unaged one. In all the scans, the fluorescence gradually decreases with increasing temperature. It is worth noting that by heating the highly aged sample (green curve), the slope of the curve drastically changes, forming a step-like pattern, in a narrow temperature range around $T_g$. The step almost disappears by heating the unaged sample; yet, after aging overnight, the step is clearly visible again, even if less marked compared to the sample aged for several weeks. A further interesting observation is that the path of fluorescence versus temperature above $T_g$ is the same for the differently aged samples, which is consistent with the achievement of the equilibrium state. In contrast, the fluorescence below $T_g$ is different and correlates well with the degree of aging of the sample at the time of the scan. Indeed, the more aged the sample (green curve), the greater its initial fluorescence intensity, while, when the thermal history was erased (black curve), the sample's initial fluorescence was lower. DSC curves reported in Figure 3B allow to appreciate that not only the step-like fluorescence decrease occurs at $T_g$, but also that its entity matches closely with that of the enthalpy relaxation peaks. These results apparently suggest that TPE, via the RIM mechanism, is sensitive to small variations in free volume since at the $T_g$ the fluorescence intensity curve presents a step-like change, whose magnitude can be attributed to the amount of free volume recovered during the transition.

Nonetheless, it is worth reminding that the measured emission intensities are proportional to the quantum yields of the dyes only if the optical system is perfectly constant during the temperature ramp. This may not be strictly true for optically complex samples, such as solid and partially transparent polymer films. Indeed, when subjected to thermal treatments, solids show defects, such as fluctuation in thickness and density, or they present areas in which the refractive index of the material itself changes. It is essential to consider such defects, as they are spots that trigger scattering and often affect emission intensity measurements. To bypass the limitations posed by the scattering phenomenon, we measured the lifetime, an absolute and quantitative parameter that is directly proportional to the quantum yield and depends only on the radiative and non-radiative decay constants. In other words, lifetime is sensitive to the RIM effect[32,33] without being affected by the scattering.

TPE lifetime was measured in the three different polymer matrices by varying the temperature (Figure 4A) and, in the case of PLGA, after different aging times (Figure 4B). Temperature Modulated DSC measurements were also carried out to quantify the enthalpy of relaxation of physically aged samples from the non-reverse heat flow curves (reported in Figure S2). The lifetime decreases during heating with a very similar trend in PVAc, PLGA, and PC, independently from the polymer $T_g$ (Figure 4A). It is worth noting that this drop has a very different trend compared to the one observed for fluorescence intensity (Figure 2). This result suggests that the direct temperature influence on the non-radiative relaxation path of TPE (i.e. on its internal conversion) is greater than the effects arising from the chain mobility changes induced by overcoming the glass transition. Also, in the case of physical aging, lifetimes are not consistent with the emission measurements (Figure 3B). From Figure 4B it is evident that, albeit the polymer free volume decreases with aging time (as proven

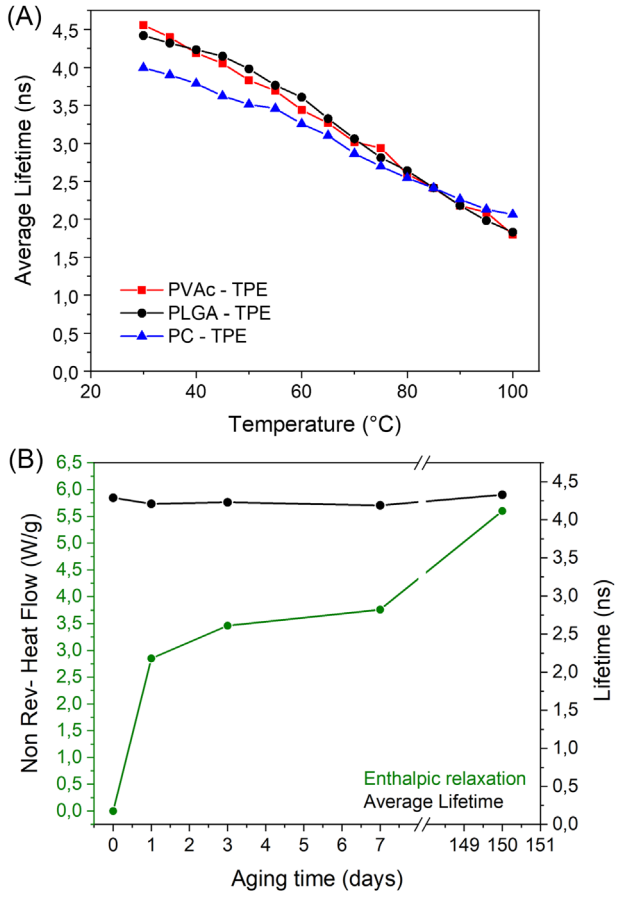


**FIGURE 4** (A) TPE average lifetime as a function of temperature when embedded in PVAc (red), PLGA (black), and PC (blue). Lifetime detection as a function of temperature in PLGA was carried out on a film containing 0.1 wt% TPE. (B) Lifetime measured at room temperature as a function of aging time in PLGA.

by the increase of the enthalpy of relaxation), TPE lifetime is not affected by polymer physical aging, thus proving that TPE is not responsive to the small changes in free volume occurring during the physical aging process, as instead previously hypothesized. As a matter of fact, the considerations made about the sensitivity of TPE on free volume and polymer $T_g$ based on the emission intensity were not confirmed by the lifetime measurements. This indicates that the observed emission variations are not the consequence of RIMs, as was instead found for another AIE dye previously investigated by some of us.[31] In the case of TPE, the source of these changes must be traced back to something else.

To assess whether the scattering can cause the emission intensity variation, we measured the transmittance (%) of films of equal thickness in the wavelength range of 300–800 nm. Figure 5 shows the average transmittance values (from multiple measurements in different areas of the sample, with error bars) obtained from differently aged PLGA-TPE samples. It is evident that, as aging time increases, the sample becomes less and less transparent. By repeating the same analysis on undoped PLGA films we observed the same behaviour, proving that the decrease in the transmittance is not ascribable to the absorbance of the dye (see Figure S3). These data corroborate previous observations demonstrating that the approaching polymer chains induce local and inhomogeneous changes in the material density during the physical aging process.[34,35] These physical defects

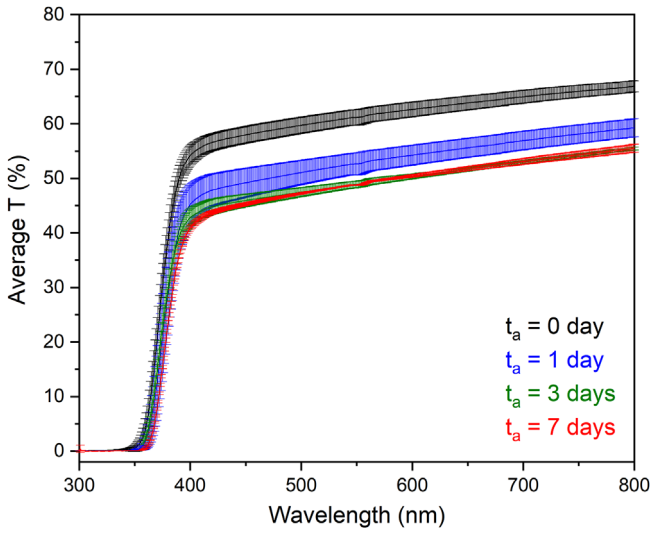


**FIGURE 5** Average transmittance (%) of PLGA-TPE after different aging times ($t_a$): unaged sample (black), $t_a$ = 1 day (blue), $t_a$ = 3 days (green), and $t_a$ = 7 days (red).

lead to the phenomenon of scattering, which, by opposing to the waveguide effect of the polymer matrix, can justify the observed enhancement in fluorescence intensity in differently aged samples (Figure 3). The same phenomenon can explain the decrease in fluorescence and under temperature variations (Figure 2). Therefore, the measurement of the lifetime, combined with transmittance, highlights that the fluorescence variations detected at the $T_g$ and in differently aged samples are ascribable to the combined effect of TPE photophysical properties temperature dependence and of the changes in the optical properties of the matrix where the TPE is dispersed, rather than to the restriction of TPE intramolecular motions.

## 2.2 | Investigation of the mechanoluminochromic response

TPE has also been explored in combination with polymer matrices to develop mechanoluminochromic materials.[29] To this aim, TPE has been dispersed in poly(styrene-*b*-butadiene-*b*-styrene) (SBS)[18] and in polydimethylsiloxane (PDMS)[25] or bonded to the main chain of a polyurethane.[22]

In this work, PVAc-TPE was tested under tensile deformation to elucidate the mechanism behind the change of emission intensity under stretching. PVAc was selected being a tough, highly deformable polymer that allows to investigate the change of sample fluorescence over a wide range of strains (mechanical data reported in Figure S4 and Table S2). As shown in Figure 6, in a first experiment, the sample was irradiated with a UV lamp (365 nm) and the tensile test was recorded with a camera (Video S1). A second experiment was then carried out similarly by replacing the UV source with a white lamp (Video S2). The comparison between the two experiments should help in assessing whether the change of fluorescence is ascribable to a change in TPE emission or rather depends on changes in the physical property of the matrix.

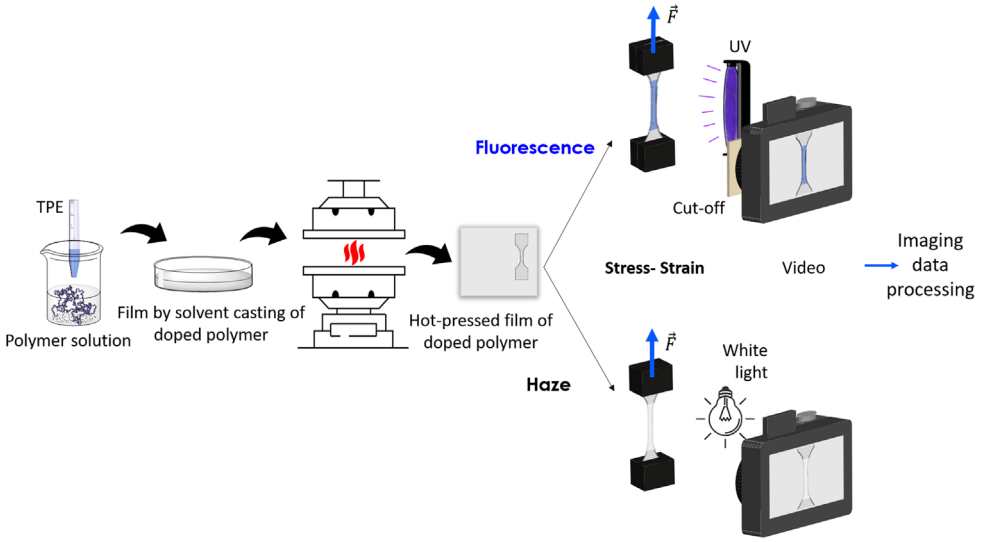


**FIGURE 6** Scheme of the experimental setup for the measurement of sample fluorescence and brightness variation during the stress–strain test: polymer films doped with TPE were obtained by solvent casting followed by hot-pressing; a dog-bone specimen was irradiated with either a UV light or a white light and the test was recorded with a camera; images were processed by analyzing greyscale intensity, using ImageJ software.

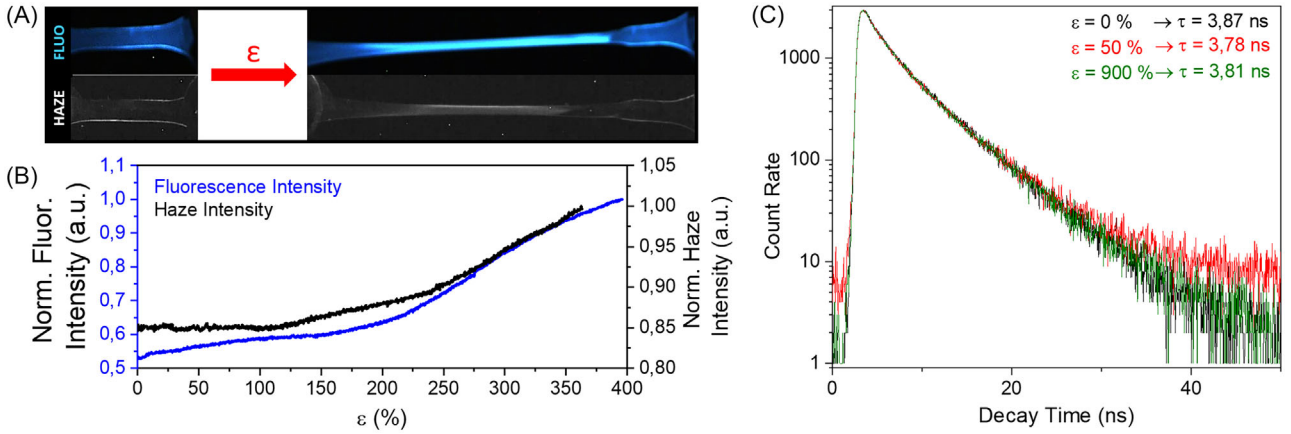


**FIGURE 7** (A) Pictures of PVAc-TPE sample at the pristine (right) and the stretched state (left) under UV (top) and transversal white light (bottom). (B) Plotting of the data obtained by the analysis of the videos recorded during stress–strain test in situ fluorescence emission (blue line) and haze (black line). (C) Fluorescence decays of PVAc-TPE stretched at different strain values (ε).

Figure 7B shows that the emission intensity of the specimen under UV light is constant up to about 100% strain and then displays a positive correlation with the strain. This result differs from previous data reported in the literature, where a negative correlation between the emission intensity and the strain was found and ascribed either to the reduced dye concentration in the excited area of the sample or to the disruption of TPE aggregates.[18,22,25] Differently from the previous studies, our analysis was not limited to the central part of the sample, but the whole sample was analyzed for the determination of the intensities. This approach reduces the effect of dye dilution on the outcomes of the analysis and can justify why emission fluorescence does not decline in our experiments. However, the observed emission increase above 100% strain is somehow unexpected, since sample stretching would suggest the occurrence of TPE disaggregation, with a consequent emission decrease owing to the reduced RIM effect.

The second experiment, performed with the white lamp, allowed to determine the change in transparency of the sample, as a gradual opaqueness was distinctly visible to the naked eye during the stretching (Figure 7A). Image analysis yielded the greyscale values of the sample versus strain, corresponding to a measurement of average scattering. It is evident that the trend of fluorescence emission (blue line in Figure 7B) and of haze (black line in Figure 7B) are very similar. This suggests that the origin of the emission increment above 100% strain lies in the emergence of scattering phenomena during the analysis, rather than an increase in the quantum yield of TPE. Scattering, indeed, can increase the observed emission intensity not only as stray light (i.e. the light at the excitation wavelength that is mistaken for emission, a contribution that can be minimized with good quality emission filters) but also due to the interruption of waveguide effect.[36] Homogeneous polymer films have a larger refractive index than air, resulting in partial waveguide of the emission light originated inside the sample, which is then transported to its edges. This can drastically reduce the amount of photons that are originated and detected in the central part of the film. The occurrence of scattering interrupts the waveguide effect, increasing the detection of the emitted

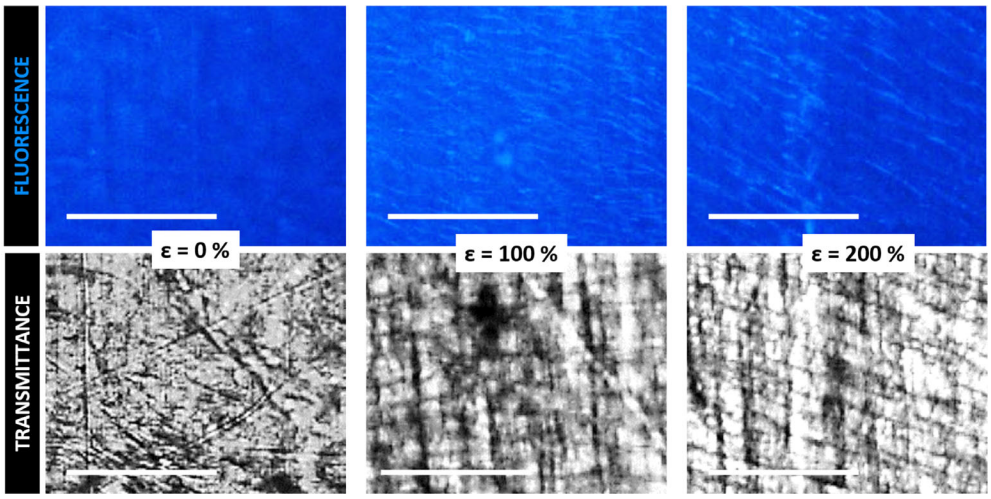


**FIGURE 8** Wide range microscope images of PVAc-TPE at 0%, 100%, and 200% strain (ε) under fluorescence (top) and transmission (bottom) microscopy. Scale bar = 100 $\mu$m.

photons nearby their origin, rather than at the edges of the film. Further evidence supporting this hypothesis is provided by the TPE lifetime—a parameter that is proportional to the quantum yield—measured at different strain values, which remains constant (lifetime values are reported in Figure 7C and differ less than 3%). It is thus confirmed that mechanical deformation, despite changing the arrangement of polymer chains, does not significantly affect the TPE mobility and its radiative decay.

The images obtained with the wide-range fluorescence optical microscope (Figure 8) better clarify what happens on the polymer sample during stretching above 100% strain. Upon deformation, microcracks are formed,[37] clearly observable during the acquisition of images at various extensions. Cracks and microcracks are usually formed during polymer use and reveal in advance permanent failure of the matrix. Notably, cracks are visible both in bright field microscopy, as dark lines, and in fluorescence imaging, where these cracks appear more emissive than the rest of the sample. Here, the waveguide effect of the polymer matrix is interrupted by these defects, which results in an only apparently increased fluorescence, which is instead due to the amount of light that is no anymore waveguided to the edges of the sample.[38,39]

In fluorescence images acquired with confocal microscopy, the microcracks formed on the sample are no longer visible (Figure 9A). This technique, indeed, minimizes waveguiding and scattering contributions since both excitation and light emission are confined in the sub-micrometric confocal volume. Therefore, in confocal microscopy, microcracks cannot act as the spot of emergence of emission light waveguided from other original spots. Finally, the FLIM technique confirmed that the lifetime of the sample does not change across the sample, not even in the proximity of the microcracks (Figure 9B), further confirming that the increase in intensity observed in wide-field microscopy and fluorescence imaging (Figures 7 and 8) arises by the interplay of waveguiding and scattering, and it is not ascribable to changes in the photophysics of the AIE probes.

## 3 | CONCLUSIONS

TPE, the simplest and most widely known AIE, was used as an additive in various polymer matrices to investigate the effects of temperature and mechanical deformation over sample optical properties with the aid of various characterization techniques that provided novel and complementary data. We confirmed previously reported phenomena, such as emission changes in correspondence of $T_g$, and we observed novel, unreported behaviour, such as emission increases in response to strain. Concerning the variations in correspondence of $T_g$, we observed an evident drop whose amplitude positively correlates to the physical aging of the sample. Accurate analysis of lifetime decays showed that these changes could only be detected via measurements of emission intensity but did not correlate with the expected variation of the fluorescence lifetime. Transmittance and microscopy measurements showed the correlation between the emergence of light scattering and the variation of emission intensity, both under thermal and mechanical stimuli, suggesting that changes in the optical transparency and the interruption of the waveguide effect could be the main cause for the observed changes in emission intensity. This has also been confirmed by confocal microscopy and FLIM investigations, which again showed the invariability of the lifetime during polymer deformation, as well as of the fluorescence intensity, when measured under the condition that the contribution of scattered light is made negligible (in confocal microscopy). Overall, TPE can be a useful probe to study thermo- and mechanochromism of polymeric matrices. Yet, measurements of an absolute fluorescence parameter such as the fluorescence lifetime are essential to discriminate between variations of the photophysical properties of the AIE dyes, related to the RIM effect, and variations that are instead related to the optical homogeneity of the polymer matrix. It is envisaged that the proposed methodology applied to other AIE dyes will facilitate a more precise identification of fluorophores that exhibit genuine sensitivity to the polymer environment.

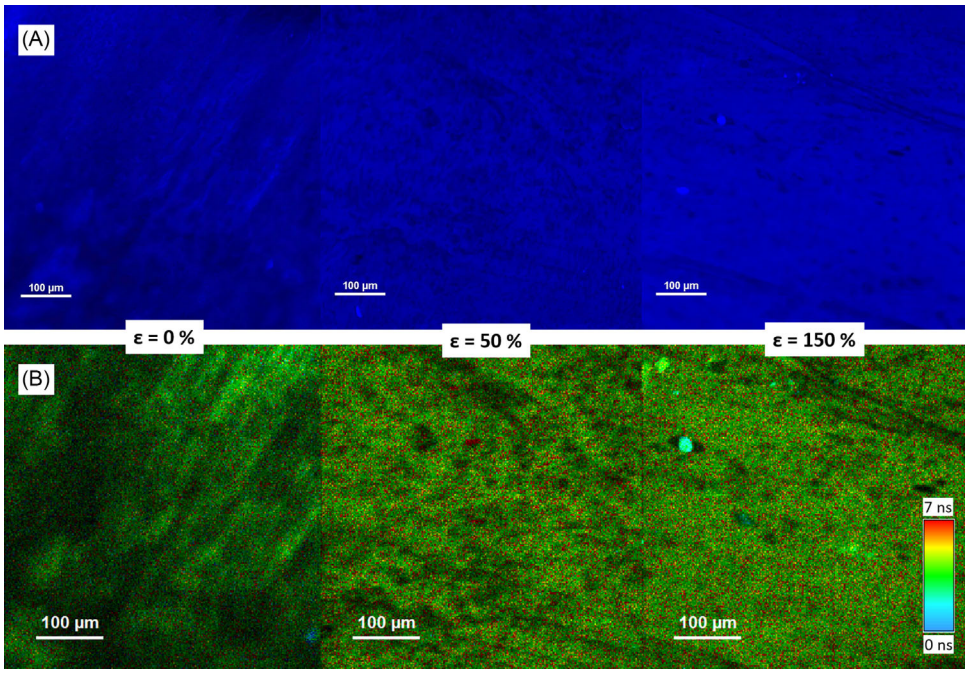


**FIGURE 9** (A) Confocal microscopy and (B) FLIM images of PVAc-TPE at 0%, 50% and 150% strain (ε).

## 4 | EXPERIMENTAL SECTION

### 4.1 | Materials

Polyvinyl acetate (PVAc, Sigma Aldrich, $M_w = 5 \times 10^5$ g/mol), and poly(lactic-*co*-glycolic acid) 75:25 mol% (PLGA, Evonik, inherent viscosity 0.71–1.0 dL/g), poly(Bisphenol A-carbonate) (PC, Sigma Aldrich, $M_w = 4.5 \times 10^4$ g/mol) were used to prepare polymeric films. Dichloromethane (DCM, ≥99.8%), Methanol (MeOH, ≥99.9%), Ethanol (EtOH, 97.2%), Tetraphenylenethylene (TPE) were provided by Sigma Aldrich and used without further purification.

### 4.2 | Film preparation

Films were obtained by solvent casting from polymeric solutions. PLGA and PC were dissolved in DCM at a concentration of 4% w/v, while PVAc was dissolved in a mixture of MeOH: EtOH = 80:20 (v/v) at 4% w/v. TPE was then added to the polymeric solutions to gain 0.1 wt% TPE in the final films of PVAc and PC and 2 wt% TPE in PLGA film. TPE concentration was set to achieve a detectable emission from the samples. After stirring until complete polymer dissolution, each mixture (70 mL) was poured into a glass petri dish ($d = 110$ mm) and left under the fume hood for solvent evaporation. The resulting films were hot-pressed at a temperature of $T_g + 100$°C and rapidly cooled to room temperature.

### 4.3 | Accelerated physical aging experiments

To investigate the effect of physical aging, all samples were thermally treated to erase their thermal history. They were heated to a temperature of $T_g + 100$°C for 10 min and then quenched using liquid nitrogen. Once prepared, samples were immediately analyzed at t0. Then they were kept at a temperature corresponding to $T_g - 15$°C, to achieve controlled aging, and analyzed after 1, 3, and 7 days.

### 4.4 | Characterization methods

Differential scanning calorimetry (DSC) was carried out using a Q2000 DSC apparatus (TA instruments) equipped with a refrigerated cooling system (RCS90). About 6 mg of sample were placed in Tzero aluminium pans and subjected to a heating scan at 20°C/min from −90°C to +150°C, quenched to −90°C, and then heated up to 150°C at 20°C/min, under nitrogen atmosphere. From this acquired data, the glass transition temperature ($T_g$) was taken at half-height of the glass transition heat capacity step in the second heating scan. Temperature-modulated DSC (TMDSC) was also performed from −20 to 150°C. The heating rate was 1°C/min, the modulation amplitude was 0.159°C and the oscillation period was 40 s. The enthalpic recovery of the aged samples was calculated as the area of the endothermal relaxation peak in the non-reversing heat flow signal.[40] Transmittance spectra were measured using a UV/vis Perkin Elmer Spectrophotometer Lambda-45 in a wavelength range from 800 to 300 nm. Fluorescence analysis under temperature was carried out by positioning the TPE-doped polymer sample (1.5 × 1.5 $cm^2$) on a heating stage (Linkam TH 600 hot stage). The sample is then irradiated with a UV light at 365 nm, while undergoing different heating and cooling scans (from RT to 150/200°C) under a controlled rate of temperature variation (5°C/min), using He flow to cool the sample (Figure 9). During these ramps, an RGB camera, with a 415 nm cut-off placed in front of the lens to filter UV light reflections, was used to capture an image sequence of the emitting sample. Data were processed using ImageJ software to obtain a graph correlating the fluorescence intensity with sample temperature. The grayscale intensity values of

the image sequence were obtained by analyzing the entire sample area and were then plotted with respect to the temperature values. An Edinburgh FLS920 fluorometer equipped with a high-speed HS773-04 photomultiplier and connected to a PCS900 PC card was used for the fluorescence lifetime measurements based on the time-correlated single photon counting technique (TCSPC). Sample lifetimes as a function of temperature were taken inserting the heating stage with the sample into the sample chamber of the instrument. Lifetimes were acquired every 5°C during a temperature ramp of 5°C/min from 25 to 100°C. A 340 nm pulsed diode laser Picoquant was used to excite the sample and the emission signal was collected at 480 nm (380 nm cut-off filter). The obtained decays were then analyzed and a good fitting obtained with a monoexponential equation resulted in an average lifetime. We used a homemade tensile tester working under strain control to determine sample lifetimes during mechanical deformation. Stress-strain tests were carried out using an Instron Testing Machine 4465 and the Series IX software package. Dog-bone-shaped samples (gage length = 20 mm, width = 5 mm, thickness = 0.1–0.3 mm) cut from each film were tested in traction mode with a load cell of 100 N. The crosshead speed was set at 10 mm/min. During mechanical tests, samples were irradiated either with a UV lamp (led at 365 nm, Thorlabs) positioned in front of the sample or with a white light positioned at 90° to the front of the sample (Figure 6). The stress–strain tests were recorded with a camera (DCC1645C—USB 2.0 CMOS, Thorlabs) placed in front of the sample. A 400 nm cut-off filter was used in front of the camera to detect fluorescence intensity and avoid stray light from UV excitation. Image J software was used to determine the sample fluorescence during the stress–strain test under UV irradiation and the change of sample haze in greyscale during the stress-strain test under white light irradiation. More in detail, the integration over a ROI was performed and taken as fluorescence or haze intensity values, respectively, to be correlated with the strain of the sample. Mechanical data are provided as average value ± standard deviation. Fluorescence microscopy was carried out using an Olympus IX 71 inverted microscope equipped with a LED (365 nm, Thorlabs) for fluorescence excitation with a bandpass excitation filter (MF390-18, Thorlabs US), then projected to the sample through reflection on a dichroic mirror (MD416, Thorlabs US) and the emission was imaged through an emission filter (wavelength interval 510 ± 42 nm) with a Basler Scout scA640-70gc CCD RGB camera for image acquisition. Images with 10X magnification were taken using the objective Olympus UPLFLN10 × 2. At the same time, using the same microscope with bright field illumination, transmission images were also obtained. Samples were also analyzed by using a Nikon A1R confocal microscope system with 20× magnification, numerical aperture, NA, 0,75 of Nikon Plan-Apo objective lens. The samples were excited by a continuous wave laser at 405 nm. The emission of the films was collected in the range of 500–620 nm. In fluorescence lifetime imaging microscopy (FLIM) a Time-correlated single photon counting (TCSPC) system of Picoquant GmbH Berlin was used with a 405 nm pulsed excitation laser at 10 MHz repetition frequency, the same dichroic mirror, a 482/35 nm bandpass emission filter, a Hybrid PMA detector and a Picoquant TimeHarp correlation board.

## ACKNOWLEDGEMENTS

The authors acknowledge MIUR through the PRIN project 20179BJNA2 for financial support.

## CONFLICT OF INTEREST STATEMENT

The authors declare no conflicts of interest.

## DATA AVAILABILITY STATEMENT

The data that support the findings of this study are available from the corresponding author upon reasonable request.

## ORCID

*Andrea Pucci* https://orcid.org/0000-0003-1278-5004
*Chiara Gualandi* https://orcid.org/0000-0002-2020-1892

## REFERENCES

1. K. M. Herbert, S. Schrettl, S. J. Rowan, C. Weder, *Macromolecules* **2017**, *50*, 8845.
2. M. Wei, Y. Gao, X. Li, M. J. Serpe, *Polym. Chem.* **2017**, *8*, 127.
3. X. Yan, F. Wang, B. Zheng, F. Huang, *Chem. Soc. Rev.* **2012**, *41*, 6042.
4. J. F. Lutz, Ö. Akdemir, A. Hoth, *J. Am. Chem. Soc.* **2006**, *128*, 13046.
5. S. Dai, P. Ravi, K. C. Tam, *Soft Matter* **2008**, *4*, 435.
6. X. Fang, H. Zhang, Y. Chen, Y. Lin, Y. Xu, W. Weng, *Macromolecules* **2013**, *46*, 6566.
7. M. Li, Q. Zhang, Y. N. Zhou, S. Zhu, *Prog. Polym. Sci.* **2018**, *79*, 26.
8. T. Wang, N. Zhang, Y. Ge, C. Wang, Z. Hang, Z. Zhang, *Macromol. Chem. Phys.* **2020**, *221*, 1900463.
9. J. Wang, B. Yue, X. Jia, R. Cao, X. Niu, H. Zhao, J. Li, L. Zhu, *Chem. Commun.* **2022**, *58*, 3517.
10. J. Luo, Z. Xie, Z. Xie, J. W. Y. Lam, L. Cheng, H. Chen, C. Qiu, H. S. Kwok, X. Zhan, Y. Liu, D. Zhu, B. Z. Tang, *Chem. Commun.* **2001**, *18*, 1740.
11. J. Mei, N. L. C. Leung, R. T. K. Kwok, J. W. Y. Lam, B. Z. Tang, *Chem. Rev.* **2015**, *115*, 11718.
12. D. D. La, S. V. Bhosale, L. A. Jones, S. V. Bhosale, *ACS Appl. Mater. Interfaces* **2018**, *10*, 12189.
13. J. Mei, Y. Hong, J. W. Y. Lam, A. Qin, Y. Tang, B. Z. Tang, *Adv. Mater.* **2014**, *26*, 5429.
14. Z. Qiu, X. Liu, J. W. Y. Lam, B. Z. Tang, *Macromol. Rapid Commun.* **2019**, *40*, 1800568.
15. S. Ge, E. Wang, J. Li, B. Z. Tang, *Macromol. Rapid Commun.* **2022**, *43*, 2200080.
16. A. Pucci, *Handb. Aggregation-Induced Emiss. Emerg. Appl.* **2022**, *3*, 57.
17. S. Bao, Q. Wu, W. Qin, Q. Yu, J. Wang, G. Liang, B. Z. Tang, *Polym. Chem.* **2015**, *6*, 3537.
18. A. Pucci, *Sensors* **2019**, *19*, 4969.
19. G. Iasilli, A. Battisti, F. Tantussi, F. Fuso, M. Allegrini, G. Ruggeri, A. Pucci, *Macromol. Chem. Phys.* **2014**, *215*, 499.
20. M. J. Robb, W. Li, R. C. R. Gergely, C. C. Matthews, S. R. White, N. R. Sottos, J. S. Moore, *ACS Cent. Sci.* **2016**, *2*, 598.
21. S. Chen, T. Han, Y. Zhao, W. Luo, Z. Zhang, H. Su, B. Z. Tang, J. Yang, *ACS Appl. Mater. Interfaces* **2020**, *12*, 4870.
22. Y. Wu, J. Hu, H. Huang, J. Li, Y. Zhu, B. Tang, J. Han, L. Li, *J. Polym. Sci. Part B Polym. Phys.* **2014**, *52*, 104.
23. Z. Qiu, W. Zhao, M. Cao, Y. Wang, J. W. Y. Lam, Z. Zhang, X. Chen, B. Z. Tang, *Adv. Mater.* **2018**, *30*, 1803924.
24. T. Bu, T. Xiao, Z. Yang, G. Liu, X. Fu, J. Nie, T. Guo, Y. Pang, J. Zhao, F. Xi, C. Zhang, Z. L. Wang, *Adv. Mater.* **2018**, *30*, 1800066.
25. B. Meng, Y. Zhang, P. C. Ma, *Macromol. Chem. Phys.* **2020**, *221*, 1900552.
26. Y. Yang, S. Zhang, X. Zhang, L. Gao, Y. Wei, Y. Ji, *Nat. Commun.* **2019**, *10*, 3165.
27. M. Y. Berezin, S. Achilefu, *Chem. Rev.* **2010**, *110*, 2641.
28. Z. Qiu, E. K. K. Chu, M. Jiang, C. Gui, N. Xie, W. Qin, P. Alam, R. T. K. Kwok, J. W. Y. Lam, B. Z. Tang, *Macromolecules* **2017**, *50*, 7620.

29. T. Han, L. Liu, D. Wang, J. Yang, B. Z. Tang, *Macromol. Rapid Commun.* **2021**, *42*, 2000311.
30. S. D. Schwab, R. L. Levy, in *Polymer Characterization*, Vol. *227* (Eds: C. D. Craver, T. Provder) American Chemical Society, **1990**, Ch.23.
31. V. A. Dini, A. Gradone, M. Villa, M. Gingras, M. L. Focarete, P. Ceroni, C. Gualandi, G. Bergamini, *Chem. Commun.* **2023**, *59*, 1465.
32. A. H. Khalid, K. Kontis, *J. Lumin.* **2011**, *131*, 1312.
33. A. J. Bur, M. G. Vangel, S. Roth, *Appl. Spectrosc.* **2002**, *56*, 174.
34. K. Takahara, H. Saito, T. Inoue, *Polymer* **1999**, *40*, 3729.
35. M. R. Tant, G. L. Wilkes, *Polym. Eng. Sci.* **1981**, *21*, 874.
36. C. Gualandi, V. A. Dini, N. Zaccheroni, D. Genovese, in *Photochemistry*, Vol. *50* (Eds: S. Crespi, S. Protti) Royal Society of Chemistry, London **2023**, Ch. 16.
37. F. Awaja, S. Zhang, M. Tripathi, A. Nikiforov, N. Pugno, *Prog. Mater. Sci.* **2016**, *83*, 536.
38. M. G. Debije, P. P. C. Verbunt, *Adv. Ener. Mat.* **2012**, *2*, 12.
39. A. Pucci, *Isr. J. Chem.* **2018**, *58*, 837.
40. L. C. Thomas, Moulated DSC Paper #5 - Measurement of Glass Transitions and Enthalpic Recovery, TA Technocal Paper, TP010, https://www.tainstruments.com/pdf/literature/TP_010_MDSC_num_5_Measurement_of_Glass_Transition_and_Enthalpic_Recovery.pdf


## SUPPORTING INFORMATION

Additional supporting information can be found online in the Supporting Information section at the end of this article.


**How to cite this article:** V. A. Dini, D. Genovese, C. Micheletti, N. Zaccheroni, A. Pucci, C. Gualandi, *Aggregate* **2023**, *4,* e373. https://doi.org/10.1002/agt2.373

Aggregate Open Access WILEY

Supporting Information

**Emission or scattering? Discriminating the origin of responsiveness in AIEgen-doped smart polymers using the TPE dye**

Valentina A. Dini, Damiano Genovese, Cosimo Micheletti, Nelsi Zaccheroni, Andrea Pucci, Chiara Gualandi*

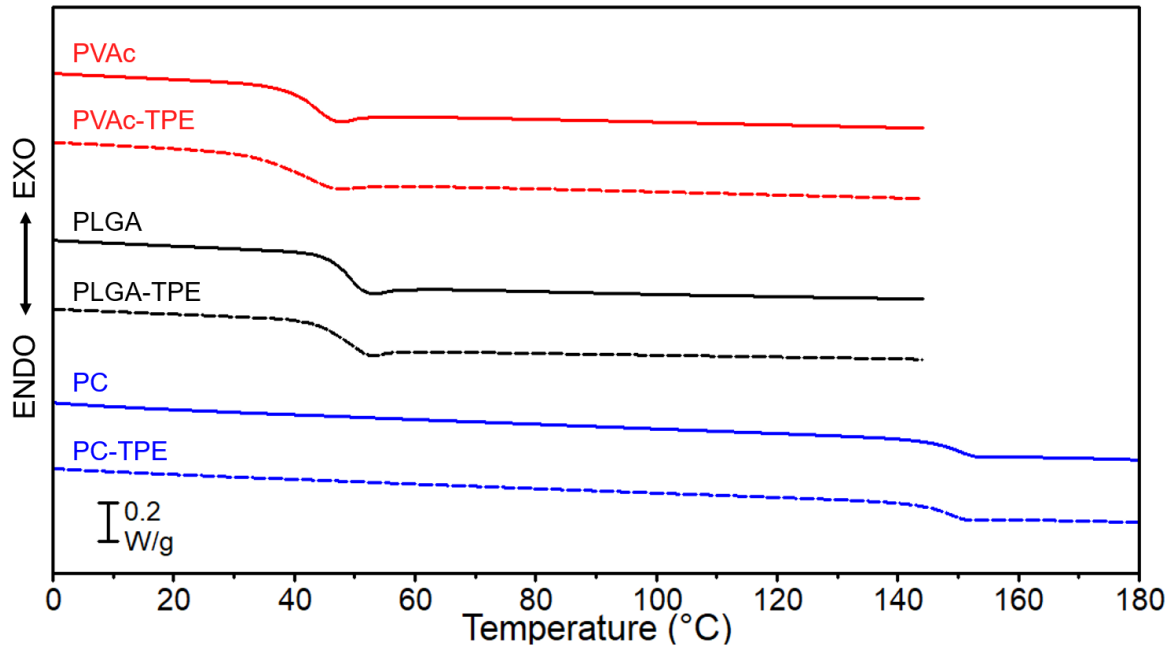


**Figure S1**. DSC second heating scans of pristine (solid line) and doped polymers (dashed line): PVAc (red), PLGA (black), and PC (blue).

**Table S1**. Thermal data of undoped and doped polymers ($T_g$ = glass transition temperature determined at the mid-point at the half height; $\Delta C_p$ = specific heat capacity variation).

| **Sample** | **$T_g$ [°C]** | **$\Delta C_p$ [J $g^{-1}$ $°C^{-1}$]** |
|---|---|---|
| PVAc | 42 | 0.51 |
| PVAc-TPE | 39 | 0.53 |
| PLGA | 48 | 0.57 |
| PLGA-TPE | 47 | 0.51 |
| PC | 149 | 0.27 |
| PC-TPE | 148 | 0.26 |

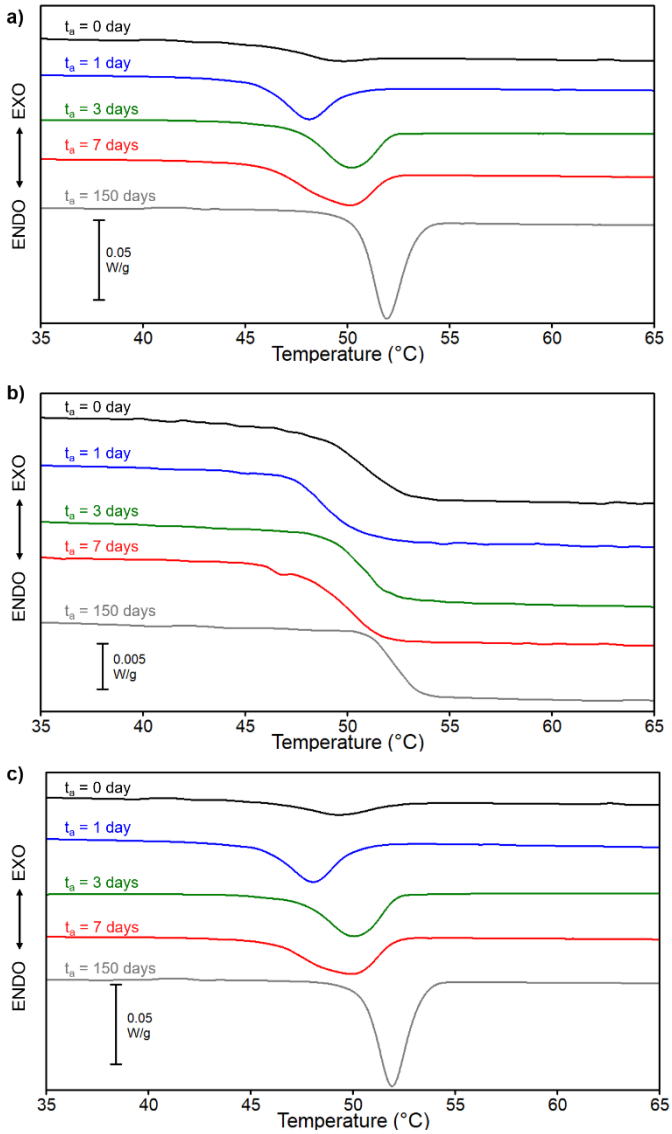


**Figure S2**. TMDSC curves of PLGA- TPE after different aging times ($t_a$): unaged (black), 1 day (blue), 3 days (green) and 7 days (red). (a) nonreversing heat flow, (b) reversing heat flow, and (c) total heat flow.

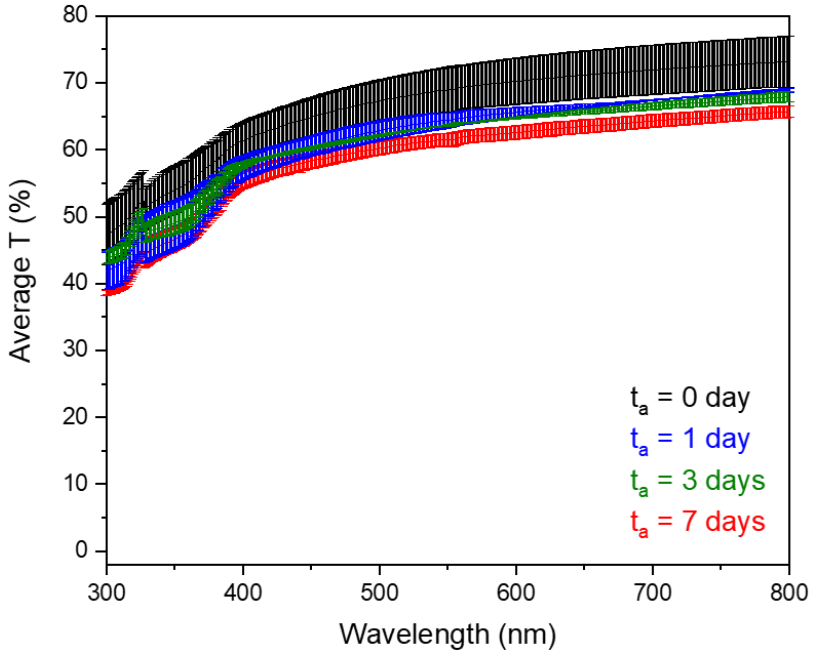


**Figure S3.** Average transmittance (%) of PLGA without TPE after different aging times ($t_a$): unaged sample (black), $t_a$ = 1 day (blue), $t_a$ = 3 days (green), and $t_a$ = 7 days (red).

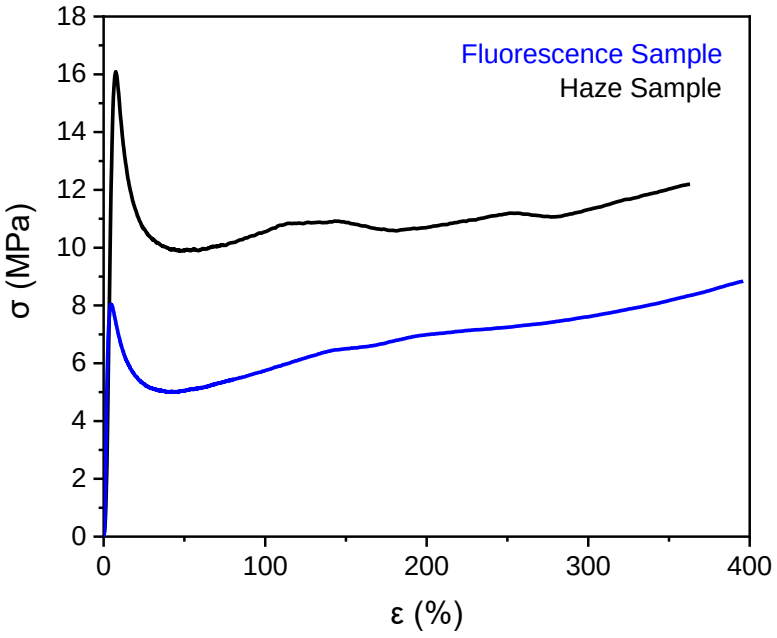


**Figure S4**. Stress-strain curves of PVAc-TPE specimens tested under UV light (blue) and white transversal light (black).

**Table S2**. Mechanical data of doped polymers (E = Young's modulus obtained from the slope of the elastic range; $\varepsilon_b$ = strain at break; $\sigma_b$ = stress at break).

| Sample | E [MPa] | $\varepsilon_b$ [%] | $\sigma_b$ [MPa] |
|---|---|---|---|
| PVAc-TPE | 620 ± 180 | 275 ± 75 | 12 ± 2 |

**Supp Video S1:** video of PVAc-TPE sample during stress-strain test under UV light. It shows the increasing of fluorescence emission during stretching.
**Supp Video S2:** video of a PVAc-TPE sample irradiated with transversal white light during the strain-stress test. It shows the increasing of sample haze during stretching.